Polynuclear Copper-Lanthanide Complexes with Amino Alcohol Ligands. Syntheses, Structures, and Magnetic and Spectroscopic Studies of $Cu^{II}(bdmmp)_2(H_2O)$, $Pr^{III}Cu^{II}(bdmmp)(bdmmpH)(\mu\text{-}OH)(hfacac)_3$, $[La^{III}Cu^{II}(bdmmp)(bdmmpH)(\mu\text{-}OH)(O_2CCF_3)_3]_2$, and $Cu^{II}_4(bdmmp)_2(\mu_4\text{-}O)(O_2CCF_3)_4$, (bdmmpH = 2,6-Bis[(dimethylamino)methyl]-4-methylphenol; hfacac = Hexafluoroacetylacetonato)

Liqin Chen,[†] Steven R. Breeze,[†] Roger J. Rousseau,[†] Suning Wang,*[,†] and Laurence K. Thompson[‡]

Department of Chemistry and Biochemistry, University of Windsor, Windsor, Ontario N9B 3P4, Canada, and Department of Chemistry, Memorial University of Newfoundland, St. John's, Newfoundland A1B 3X7, Canada

Received May 19, 1994[⊗]

The syntheses of polynuclear copper(II)-lanthanide(III) complexes using the 2,6-bis[(dimethylamino)methyl]-4-methylphenolato ligand (bdmmp) have been investigated. The reaction of $Cu(OCH_3)_2$ with 2 equiv of bdmmpH in THF yields a mononuclear copper complex $Cu(bdmmp)_2(H_2O)$ (**1**), which subsequently reacts with 1 equiv of $Pr(hfacac)_3$ or $La(O_2CCF_3)_3$ (hfacac = hexafluoroacetylacetonato) to produce two heteronuclear complexes $Pr^{III}Cu^{II}(bdmmp)(bdmmpH)(OH)(hfacac)_3$ (**2**) and $[La^{III}Cu^{II}(bdmmp)(bdmmpH)(OH)(O_2CCF_3)_3]_2$ (**3**). The reaction of $Cu(OCH_3)_2$, $Cu(O_2CCF_3)_2$, bdmmpH, and H_2O in a 1:1:1:0.5 ratio in THF yields a tetranuclear copper complex $Cu_4(bdmmp)_2(\mu_4\text{-}O)(O_2CCF_3)_4$ (**4**). The structures of compounds **1**-**4** have been determined by single-crystal X-ray diffraction analysis. Compound **1** crystallizes in the monoclinic crystal space group $C2/c$, with $a = 17.443(8)$ Å, $b = 9.510(3)$ Å, $c = 20.459(9)$ Å, $\beta = 122.89(3)°$, $V = 2849(2)$ Å^3, and $Z = 4$. Compound **2** crystallizes in the monoclinic space group $P2_1/n$, with $a = 14.304(8)$ Å, $b = 19.122(6)$ Å, $c = 20.059(4)$ Å, $\beta = 100.21(3)°$, $V = 5399(3)$ Å^3, and $Z = 4$. Compound **3** crystallizes in the triclinic space group $P\bar{1}$, with $a = 13.106(6)$ Å, $b = 17.15(1)$ Å, $c = 11.152(6)$ Å, $\alpha = 97.14(4)°$, $\beta = 108.48(4)°$, $\gamma = 93.85(4)°$, $V = 2343(2)$ Å^3, and $Z = 1$. Compound **4** crystallizes in the orthorhombic space group $P2_12_12_1$, with $a = 18.408(7)$ Å, $b = 22.88(1)$ Å, $c = 10.598(5)$ Å, $V = 4464(2)$ Å^3, and $Z = 4$. The magnetic properties of these compounds have been examined by variable-temperature magnetic susceptibility measurements. The magnetism of compound **2** is dominated by the paramagnetism of the Pr(III) ion, while the magnetism of **4** is dominated by antiferromagnetic exchanges of the Cu(II) ions with $J_1 = -101$ cm^{-1}, $J_2 = -101$ cm^{-1}, $J_3 = -45$ cm^{-1}, $J_4 = 3$ cm^{-1}, and $g = 2.02$. UV-vis spectroscopic studies revealed that compound **1** has an intense ligand → metal charge transfer band at $\lambda = 427$ nm. Molecular orbital analysis on the electronic structure of **1** by extended Hückel MO methods indicates that this absorption band is mainly due to the transitions of the π orbitals of the phenoxy ligand to the singly occupied $d_{x^2-y^2}$ orbital of the copper ion.

Introduction

Polynuclear copper-lanthanide complexes have attracted much attention, mostly due to their potential applications in superconducting ceramic and magnetic materials as well as models for theoretical investigation on the magnetic exchange involving d and f electrons.[1] In addition, we reported recently that heteronuclear Cu(II)-Ln(III) complexes can also have unusual reactivities toward certain organic substrates.[2] We have been investigating the synthesis of heteronuclear Cu-Ln complexes by using amino alcohols as bridging ligands. Several heteronuclear Cu-Ln complexes with the 1,3-bis(dimethylamino)-2-propanolato ligand have been obtained previously.[2,3] It is, however, usually difficult to isolate these complexes from solution due to their high solubility and tendency to form oily material in common organic solvents,[2,3] thus making the investigation of their physical and chemical properties difficult. We have, therefore, explored the synthesis of Cu-Ln complexes with amino alcohol ligands such as 2,6-bis[(dimethylamino)-methyl]-4-methylphenol (bdmmpH). Several heteronuclear Cu-Ln complexes have been obtained in good yield by using the bdmmpH ligand. The details of the syntheses, structures, and physical properties of these compounds and related copper(II) complexes are reported herein.

[†] University of Windsor.
[‡] Memorial University of Newfoundland.
[⊗] Abstract published in *Advance ACS Abstracts*, January 1, 1995.

(1) (a) *Better Ceramics through Chemistry, IV*; Zelinski, B. J. J., Brinker, C. J., Clark, D. E., Ulrich, D. R., Eds.; Material Research Society: Pittsburgh, PA, 1990. (b) Rupich, M. W.; Lagos, B.; Hachey, J. P. *Appl. Phys. lett.* **1989**, *55*, 2447. (c) Bouayad, A.; Brouca-Cabarrecq, C.; Trombe, J.-C. *Inorg. Chim. Acta* **1992**, *195*, 193. (d) Guillou, O.; Oushoorn, R. L.; Kahn, O.; Boukekeur, K.; Betail, P. *Angew. Chem., Int. Ed. Engl.* **1992**, *31*, 626. (e) Blake, A. J.; Milne, P. E. Y.; Thornton, P.; Winpenny, R. E. P. *Angew. Chem., Int. Ed. Engl.* **1991**, *30*, 1139. (f) Blake, A. J.; Gould, R. O.; Milne, P. E. Y.; Winpenny, R. E. P. *J. Chem. Soc., Chem. Commun.* **1991**, 1453. (g) Sakamoto, M.; Takagi, M.; Ishimori, T.; Okawa, H. *Bull. Chem. Soc. Jpn.* **1988**, *61*, 1613. (h) Wang, S.; Pang, Z.; Wagner, M. J. *Inorg. Chem.* **1992**, *31*, 5381. (i) Benelli, C.; Caneschi, A.; Gatteschi, D.; Guillou, O.; Pardi, L. *Inorg. Chem.* **1990**, *29*, 1750. (j) Goodgame, D. M. L.; Williams, D. J.; Winpenny, R. E. P. *Polyhedron* **1989**, *8*, 1531.
(2) Wang, S.; Pang, Z.; Smith, K. D. L. *Inorg. Chem.* **1993**, *32*, 4992.
(3) Wang, S.; Pang, Z.; Smith, K. D. L.; Wagner, M. J. *J. Chem. Soc., Dalton Trans.* **1994**, 955.

0020-1669/95/1334-0454$09.00/0

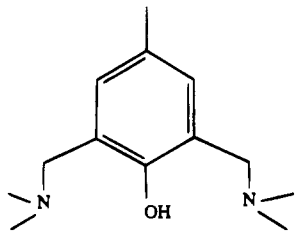

bdmmpH

Experimental Section

All reactions were carried out under a dry nitrogen atmosphere by using the standard Schlenk line techniques. $Pr(hfacac)_3$ was purchased from Strem Chemicals. $Cu(OCH_3)_2$, trifluoroacetic acid, and 4-methylphenol were obtained from Aldrich Chemicals Co. Solvents were freshly distilled prior to use. 2,6-Bis[(dimethylamino)methyl]-4-methylphenol (bdmmpH) was synthesized via a procedure described in the literature.[4] $La(O_2CCF_3)_3$ was synthesized by the reaction of La_2O_3 with HO_2CCF_3 in THF and isolated as a colorless microcrystalline solid through repeated crystallization and filtration processes. UV−vis spectra were recorded on a Gilford Response UV-VIS spectrometer interfaced with an IBM computer. IR spectra were recorded on a Nicolet FTIR-5DX spectrometer with samples prepared as KBr pellets. Variable-temperature magnetic susceptibility data were obtained in the range 5−300 K using an Oxford Instruments superconducting Faraday susceptometer with a Sartorius 4432 microbalance. Susceptibility data were corrected for diamagnetism (Pascal corrections), for temperature-independent paramagnetism, and for the presence of monomer impurity. $HgCo(NCS)_4$ was used as a calibration standard.

Synthesis of Cu(bdmmp)$_2$(H$_2$O) (1). A mixture of $Cu(OCH_3)_2$ (100 mg, 0.80 mmol) and bdmmpH (354 mg, 1.60 mmol) in 15 mL of THF was stirred at 23 °C for 20 h. The solution was then filtered and concentrated to about 7 mL *in vacuo*. Excess hexane was added to crystallize the product. Dark brown crystals of **1** solvated by THF with the formula of $Cu(bdmmp)_2(H_2O)(THF)$ were obtained (280 mg, 0.468 mmol, 59% yield). The nonsolvated crystals of **1** can be obtained when excess hexane is used. Anal. Calcd for the vacuum-dried sample $C_{26}H_{44}N_4O_3Cu$: C, 59.35; H, 8.81; N, 10.65. Found: C, 58.79; H, 8.71; N, 11.10. Mp: 96−97 °C dec. IR (KBr, cm^{-1}): 1003 w, 1035 w, 1174 w, 1260 w, 1313 s, 1343 w, 1467 s, 1630 m. UV−vis (1.25×10^{-4} M, THF; λ_{max}, nm): 217 (ϵ = 27 840 M^{-1} cm^{-1}), 247 (ϵ = 18 080 M^{-1} cm^{-1}), 305 (ϵ = 12 710 M^{-1} cm^{-1}), 427 (ϵ = 1160 M^{-1} cm^{-1}).

Synthesis of PrCu(bdmmpH)(bdmmp)(μ-OH)(hfacac)$_3$ (2). Method A. $Cu(OCH_3)_2$ (50 mg, 0.40 mmol) and 178 mg of bdmmpH (0.80 mmol) were added to a flask containing 10 mL of THF. A brown solution was obtained. After the solution was stirred for 4 h at 23 °C, $Pr(hfacac)_3$ (305 mg, 0.40 mmol) was added. After being stirred for additional 4 h, the solution was filtered and concentrated to about 5 mL *in vacuo*. After standing at 23 °C for a few days, the mixture yielded dark green crystals of **2** (350 mg, 0.27 mmol, 68% yield). The crystal of **2** decomposes at 163 °C. Anal. Calcd for $C_{41}H_{47}N_4O_{12}F_{18}CuPr$: C, 38.29; H, 3.68; N, 4.36. Found: C, 38.35; H, 3.88; N, 4.50. IR (KBr, cm^{-1}): 1097 w, 1142 vs, 1203 s, 1255 s, 1317 w, 1441 w, 1472 m, 1525 m, 1630 m, 1656 s, 1673 m. UV−vis (1.0×10^{-4} M, THF; λ_{max}, nm): 215 (ϵ = 29 330 M^{-1} cm^{-1}), 238 (ϵ = 15 350 M^{-1} cm^{-1}), 303 (ϵ = 30 170 M^{-1} cm^{-1}), 428 (ϵ = 970 M^{-1} cm^{-1}).

Method B. Compound **1** (100 mg, 0.190 mmol) was dissolved in 15 mL of THF, and 145 mg of $Pr(hfacac)_3$ (0.190 mmol) was added. The dark brown solution became light brown. The mixture was stirred for 20 h at 23 °C. After filtration, the solution was concentrated to about 2 mL, and 1 mL of hexane was added to crystallize the product. After being kept at 0 °C for a few days, the mixture yielded dark green crystals of **2** (115 mg, 0.089 mmol, yield 47%).

Synthesis of [LaCu(bdmmpH)(bdmmp)(μ-OH)(O$_2$CCF$_3$)$_3$]$_2$ (3). Method A. $Cu(OCH_3)_2$ (75 mg, 0.60 mmol) was added to a flask containing 10 mL of THF. 2,6-Bis[(dimethylamino)methyl]-4-methylphenol (267 mg, 1.20 mmol) was added. A brown solution was obtained. After the solution was stirred for 4 h at 23 °C, $La(O_2CCF_3)_3$ (287 mg, 0.60 mmol) was added. The solution color changed to greenish brown. After being stirred for additional 4 h, the solution was filtered and concentrated to about 5 mL *in vacuo*. Excess hexane was added to crystallize the product. After a few days of standing at 23 °C, dark green crystals of **3** were collected (195 mg, 0.20 mmol, 33% yield). The crystal of **3** decomposes at 155 °C. Anal. Calcd for $C_{64}H_{88}N_8O_{18}F_{18}Cu_2La_2$: C, 38.31; H, 4.39; N, 5.59. Found for the dried sample: C, 38.53; H, 4.40; N, 5.46. IR (KBr, cm^{-1}): 1136 s, 1205 vs, 1247 m, 1278 w, 1315 m, 1342 w, 1428 w, 1475 s, 1680 s, 1719 s. UV−vis (1.25×10^{-4} M_{Cu}, THF; λ_{max}, nm): 217 (ϵ = 24 320 M_{Cu}^{-1} cm^{-1}), 233 (ϵ = 13 600 M_{Cu}^{-1} cm^{-1}), 288 (ϵ = 9440 M_{Cu}^{-1} cm^{-1}), 422 (ϵ = 460 M_{Cu}^{-1} cm^{-1}), 685 (ϵ = 100 M_{Cu}^{-1} cm^{-1}).

Table 1. Crystallographic Data

	1	2	3	4
Formula	$C_{26}H_{44}N_4O_3Cu$	$C_{41}H_{47}N_4O_9F_{18}CuPr$	$C_{70}H_{102}N_8O_{18}F_{18}Cu_2La_2$	$C_{34}H_{42}N_4O_{11}F_{12}Cu_4$
fw	524.2	1286.3	2090.5	1164.9
space group	$C2/c$	$P2_1/n$	$P\bar{1}$	$P2_12_12_1$
a, Å	17.443(8)	14.304(8)	13.106(6)	18.408(7)
b, Å	9.510(3)	19.122(6)	17.15(1)	22.88(1)
c, Å	20.459(9)	20.059(4)	11.152(6)	10.598(5)
α, deg	90	90	97.14(4)	90
β, deg	122.89(3)	100.21(3)	108.48(4)	90
γ, deg	90	90	93.85(4)	90
V, Å^3	2849(2)	5399(3)	2343(2)	4464(2)
Z	4	4	1	4
d_{calcd}, g cm^{-3}	1.222	1.582	1.481	1.733
μ, cm^{-1}	7.98	13.96	14.34	19.88
λ(Mo Kα), Å	0.710 69	0.710 69	0.710 69	0.710 69
T, °C	23	23	23	23
R^a	0.038	0.069	0.058	0.076
$R_w{}^b$	0.029	0.054	0.052	0.059

$^a R = \sum||F_o| - |F_c||/\sum|F_o|$. $^b R_w = [(\sum w(|F_o| - |F_c|)^2/\sum wF_o^2]^{1/2}$, where $w = 1/\sigma^2(F_o)$.

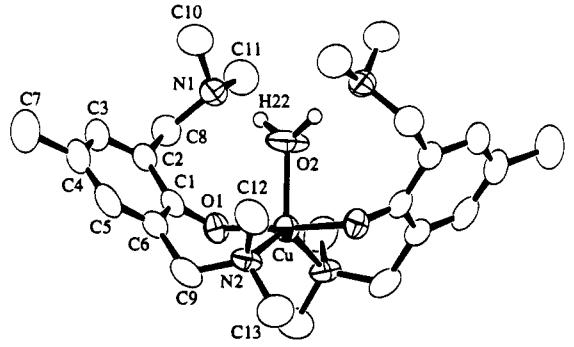

Figure 1. ORTEP diagram showing the molecular structure of **1** with labeling scheme and 50% thermal ellipsoids.

Scheme 1

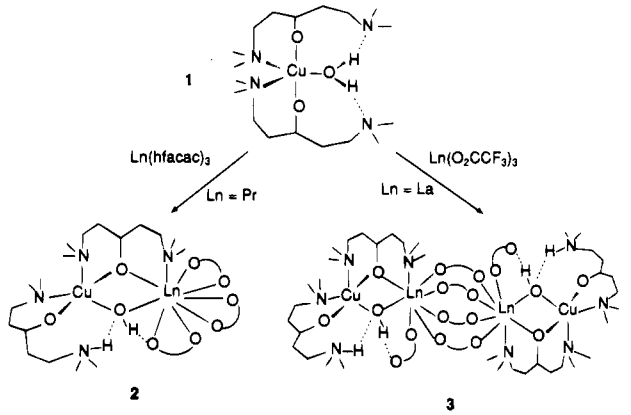

(4) van der Schaaf, P. A.; Jastrzebski, J. T. B. H.; Hogerheide, M. P.; Smeets, W. J. J.; Spek, A. L.; Boersma, J.; Van koten, G. *Inorg. Chem.* **1993**, *32*, 4111.

Table 2

(a) Positional and Thermal Parameters (B_{eq}) for **1**

atom	*x*	*y*	*z*	B_{eq},[a] Å^2	atom	*x*	*y*	*z*	B_{eq},[a] Å^2
Cu	0	0.18079(9)	$-1/4$	3.06(3)	C(5)	0.0427(3)	0.2342(5)	−0.4489(2)	4.2(2)
O(1)	0.1123(2)	0.1873(3)	−0.2470(1)	3.4(1)	C(6)	0.0467(3)	0.1809(5)	−0.3836(2)	3.3(2)
O(2)	0	0.3969(4)	$-1/4$	8.6(3)	C(7)	0.0944(3)	0.4028(6)	−0.5139(3)	6.6(3)
N(1)	0.1594(2)	0.5296(4)	−0.2125(2)	3.6(2)	C(8)	0.2136(3)	0.4353(5)	−0.2282(2)	3.9(2)
N(2)	−0.0713(2)	0.0876(4)	−0.3631(2)	3.5(2)	C(9)	−0.0083(3)	0.0571(5)	−0.3888(3)	4.3(2)
C(1)	0.1045(3)	0.2427(5)	−0.3115(2)	3.1(2)	C(10)	0.1291(3)	0.6526(5)	−0.2630(3)	5.3(2)
C(2)	0.1563(3)	0.3602(5)	−0.3051(3)	3.2(2)	C(11)	0.2124(4)	0.5753(5)	−0.1308(3)	5.8(3)
C(3)	0.1512(3)	0.4088(5)	−0.3718(3)	4.0(2)	C(12)	−0.1419(3)	0.1881(6)	−0.4170(2)	4.9(2)
C(4)	0.0963(3)	0.3468(6)	−0.4428(3)	4.3(2)	C(13)	−0.1163(3)	−0.0410(5)	−0.3623(3)	5.5(2)

(b) Positional and Thermal Parameters (B_{eq}) for **2**

atom	*x*	*y*	*z*	B_{eq}, Å^2	atom	*x*	*y*	*z*	B_{eq}, Å^2
Pr	0.67039(5)	0.20796(4)	0.03655(4)	3.32(3)	C(14)	0.8848(9)	0.4202(8)	−0.0544(7)	4.2(7)
Cu	0.8513(1)	0.27589(8)	−0.04447(8)	3.26(7)	C(15)	0.8813(9)	0.4771(8)	−0.0120(8)	4.3(7)
O(1)	0.7540(5)	0.3130(4)	0.0092(4)	3.6(4)	C(16)	0.846(1)	0.5409(8)	−0.039(1)	5.2(8)
O(2)	0.7693(5)	0.1934(4)	−0.0489(4)	3.3(4)	C(17)	0.817(1)	0.552(1)	−0.105(1)	6(1)
O(3)	0.9259(5)	0.3594(5)	−0.0287(4)	3.7(4)	C(18)	0.821(1)	0.497(1)	−0.1494(8)	5.5(9)
O(4)	0.8242(5)	0.2094(5)	0.1204(4)	4.4(4)	C(19)	0.856(1)	0.4289(8)	−0.1240(8)	4.6(8)
O(5)	0.7383(6)	0.0887(4)	0.0552(5)	4.7(5)	C(20)	0.779(2)	0.621(1)	−0.139(1)	10(1)
O(6)	0.6523(8)	0.1508(7)	0.1481(6)	8.0(7)	C(21)	0.855(1)	0.3676(8)	−0.1709(7)	4.8(8)
O(7)	0.6310(6)	0.2958(6)	0.1210(4)	5.1(5)	C(22)	0.907(1)	0.4646(8)	0.0620(8)	5.3(8)
O(8)	0.5579(6)	0.2963(5)	−0.0235(4)	4.8(5)	C(23)	0.801(1)	0.2526(8)	−0.2037(7)	6.1(8)
O(9)	0.5064(7)	0.1838(5)	0.0505(5)	4.6(5)	C(24)	0.698(1)	0.3311(7)	−0.1605(7)	5.0(7)
N(1)	0.5723(7)	0.1278(6)	−0.0773(5)	3.6(5)	C(25)	0.748(1)	0.4560(8)	0.0895(8)	6(1)
N(2)	0.9769(6)	0.2170(6)	−0.0237(5)	3.8(5)	C(26)	0.875(1)	0.3905(9)	0.156(1)	8(1)
N(3)	0.7972(7)	0.3071(5)	−0.1555(5)	3.9(5)	C(27)	0.931(1)	0.196(1)	0.2200(8)	7(1)
N(4)	0.8365(8)	0.4187(6)	0.0870(6)	4.2()6)	C(28)	0.865(1)	0.1646(9)	0.1600(7)	4.1(7)
C(1)	0.7946(9)	0.1317(7)	−0.0756(6)	3.3(6)	C(29)	0.8557(9)	0.093(1)	0.1530(7)	4.8(8)
C(2)	0.7236(9)	0.0933(7)	−0.1164(7)	3.7(6)	C(30)	0.793(1)	0.0607(8)	0.1007(7)	4.0(7)
C(3)	0.749(1)	0.0306(8)	−0.1420(7)	4.6(7)	C(31)	0.789(2)	−0.020(1)	0.098(1)	7(1)
C(4)	0.840(1)	0.0044(7)	−0.1306(7)	4.5(7)	C(32)	0.615(2)	0.100(2)	0.255(2)	21(3)
C(5)	0.909(1)	0.0427(8)	−0.0864(7)	4.4(7)	C(33)	0.616(1)	0.158(1)	0.194(1)	7(1)
C(6)	0.8867(8)	0.1054(7)	−0.0579(6)	3.5(6)	C(34)	0.593(2)	0.230(2)	0.214(1)	11(2)
C(7)	0.865(1)	−0.064(1)	−0.1629(9)	8(1)	C(35)	0.598(2)	0.292(1)	0.170(1)	11(2)
C(8)	0.6251(9)	0.1221(7)	−0.1344(6)	3.7(6)	C(36)	0.567(2)	0.369(2)	0.198(1)	11.1(7)
C(9)	0.9567(8)	0.1421(8)	−0.0054(6)	3.9(6)	C(37)	0.349(2)	0.179(1)	0.081(1)	9.7(6)
C(10)	0.480(1)	0.1590(8)	−0.1066(7)	4.9(8)	C(38)	0.437(1)	0.209(1)	0.053(1)	9(1)
C(11)	0.553(1)	0.0603(8)	−0.0548(7)	4.9(8)	C(39)	0.418(2)	0.283(2)	0.019(1)	13(2)
C(12)	1.029(1)	0.216(1)	−0.082(1)	7(1)	C(40)	0.486(2)	0.322(1)	−0.015(1)	8(1)
C(13)	1.038(1)	0.2452(8)	0.0358(8)	5.7(8)	C(41)	0.433(2)	0.399(2)	−0.061(2)	16(1)

(c) Positional and Thermal Parameters (B_{eq}) for **3**

atom	*x*	*y*	*z*	B_{eq}, Å^2	atom	*x*	*y*	*z*	B_{eq}, Å^2
La	0.45426(8)	0.13220(6)	0.4746(1)	2.91(4)	C(10)	0.702(1)	0.285(1)	0.882(2)	5.8(4)
Cu	0.3234(1)	0.2733(1)	0.6170(2)	3.9(1)	C(11)	0.591(1)	0.186(1)	0.933(2)	5.8(4)
O(1)	0.2941(6)	0.1999(5)	0.4572(8)	3.4(4)	C(12)	0.398(1)	0.402(1)	0.475(2)	5.6(4)
O(2)	0.3647(7)	0.3348(5)	0.7823(8)	4.0(4)	C(13)	0.207(1)	0.389(1)	0.428(2)	7.0(5)
O(3)	0.4825(6)	0.2478(5)	0.6421(8)	3.1(4)	C(14)	0.262(1)	0.2025(8)	0.194(1)	3.9(3)
O(4)	0.5737(8)	0.2274(6)	0.426(1)	5.1(5)	C(15)	0.172(1)	0.1809(8)	0.244(1)	3.6(3)
O(5)	0.650(1)	0.3356(7)	0.569(1)	7.8(7)	C(16)	0.068(1)	0.161(1)	0.159(2)	5.3(4)
O(6)	0.4092(7)	0.0826(6)	0.663(1)	4.7(5)	C(17)	−0.015(1)	0.140(1)	0.204(2)	5.5(4)
O(7)	0.4691(7)	−0.0351(6)	0.6507(9)	4.7(5)	C(18)	−0.138(2)	0.121(1)	0.106(2)	9.3(6)
O(8)	0.3129(7)	0.0130(5)	0.399(1)	4.0(4)	C(19)	0.007(1)	0.137(1)	0.333(2)	4.9(4)
O(9)	0.3607(7)	−0.1109(6)	0.3729(9)	4.4(4)	C(20)	0.110(1)	0.1572(8)	0.422(1)	3.6(3)
N(1)	0.5947(9)	0.2626(7)	0.888(1)	4.0(5)	C(21)	0.193(1)	0.1803(7)	0.373(1)	3.1(3)
N(2)	0.312(1)	0.3884(7)	0.529(1)	4.5(6)	C(22)	0.136(1)	0.1470(9)	0.555(1)	4.1(3)
N(3)	0.3430(8)	0.1447(6)	0.209(1)	3.4(5)	C(23)	0.423(1)	0.176(1)	0.152(2)	5.8(4)
N(4)	0.1848(9)	0.2225(7)	0.646(1)	3.7(5)	C(24)	0.289(1)	0.070(1)	0.131(2)	5.8(4)
C(1)	0.563(1)	0.3285(9)	0.974(1)	4.4(3)	C(25)	0.215(1)	0.205(1)	0.777(2)	6.4(4)
C(2)	0.542(1)	0.3998(9)	0.9010(1)	4.1(3)	C(26)	0.101(1)	0.276(1)	0.635(2)	5.8(4)
C(3)	0.614(1)	0.4666(9)	0.945(1)	4.2(3)	C(27)	0.641(1)	0.283(1)	0.479(2)	5.2(4)
C(4)	0.597(1)	0.529(1)	0.881(2)	4.9(4)	C(28)	0.736(2)	0.296(2)	0.426(3)	6.8(6)
C(5)	0.677(1)	0.603(1)	0.918(2)	6.8(5)	C(29)	0.418(1)	0.017(1)	0.689(2)	4.9(4)
C(6)	0.500(1)	0.5251(9)	0.777(1)	4.5(4)	C(30)	0.353(2)	−0.011(2)	0.770(2)	6.2(5)
C(7)	0.423(1)	0.461(1)	0.742(1)	4.3(3)	C(31)	0.296(1)	−0.061(1)	0.371(1)	3.4(3)
C(8)	0.439(1)	0.397(1)	0.810(1)	4.2(3)	C(32)	0.174(1)	−0.095(1)	0.324(2)	5.9(4)
C(9)	0.321(1)	0.456(1)	0.632(2)	5.5(4)					

(d) Positional and Thermal Parameters (B_{eq}) for **4**

atom	*x*	*y*	*z*	B_{eq}, Å^2	atom	*x*	*y*	*z*	B_{eq}, Å^2
Cu(1)	0.5820(1)	0.1072(1)	0.7017(2)	2.2(1)	C(9)	0.676(1)	0.098(1)	0.488(2)	4.3(6)
Cu(2)	0.5398(1)	0.1498(1)	0.9519(2)	2.3(1)	C(10)	0.699(1)	0.029(1)	0.648(2)	3.8(5)

Table 2 (Continued)

atom	x	y	z	B_{eq}, Å^2	atom	x	y	z	B_{eq}, Å^2
Cu(3)	0.4378(1)	0.1817(1)	0.7044(2)	2.0(1)	C(11)	0.654(1)	0.1259(9)	1.127(2)	2.7(4)
Cu(4)	0.4205(1)	0.0675(1)	0.8266(2)	2.1(1)	C(12)	0.628(1)	0.233(1)	1.083(2)	4.7(6)
O(1)	0.4948(5)	0.1265(5)	0.801(1)	1.9(6)	C(13)	0.553(1)	0.174(1)	1.220(2)	6.9(7)
O(2)	0.6274(7)	0.1321(5)	0.854(1)	2.6(3)	C(14)	0.290(1)	0.1294(9)	0.713(2)	3.1(4)
O(3)	0.3644(6)	0.1205(5)	0.727(1)	2.0(3)	C(15)	0.263(1)	0.169(1)	0.628(2)	2.6(4)
O(4)	0.4544(8)	0.1938(7)	1.014(1)	4.5(4)	C(16)	0.187(1)	0.176(1)	0.618(2)	3.0(4)
O(5)	0.3876(8)	0.1116(8)	1.025(2)	5.4(4)	C(17)	0.142(1)	0.141(1)	0.694(2)	3.4(5)
O(6)	0.5295(7)	0.0618(6)	0.577(1)	3.0(3)	C(18)	0.168(1)	0.1021(8)	0.780(2)	2.2(4)
O(7)	0.4676(8)	0.1372(6)	0.504(1)	3.7(3)	C(19)	0.243(1)	0.0939(8)	0.793(2)	2.3(4)
O(8)	0.5039(7)	0.2465(6)	0.738(1)	2.5(3)	C(20)	0.058(1)	0.151(1)	0.679(2)	6.0(6)
O(9)	0.5984(7)	0.2133(6)	0.625(1)	4.5(9)	C(21)	0.266(1)	0.050(1)	0.885(2)	3.7(5)
O(10)	0.4900(7)	0.0043(6)	0.858(2)	3.8(8)	C(22)	0.322(1)	−0.021(1)	0.744(2)	4.6(6)
O(11)	0.541(1)	0.0472(8)	1.026(2)	6(1)	C(23)	0.348(1)	−0.026(1)	0.962(2)	4.5(6)
N(1)	0.679(1)	0.0876(8)	0.615(2)	3.4(4)	C(24)	0.314(1)	0.2015(8)	0.541(2)	2.1(4)
N(2)	0.5995(7)	0.1750(6)	1.105(1)	1.5(3)	C(25)	0.338(1)	0.275(1)	0.689(2)	3.7(5)
N(3)	0.3363(8)	0.0129(7)	0.856(1)	2.4(3)	C(26)	0.410(1)	0.267(1)	0.502(2)	3.8(5)
N(4)	0.3703(8)	0.2324(7)	0.609(1)	2.2(3)	C(27)	0.400(1)	0.162(1)	1.043(2)	3.7(5)
C(1)	0.699(1)	0.1290(9)	0.899(2)	2.4(4)	C(28)	0.336(2)	0.196(2)	1.114(3)	6.7(8)
C(2)	0.713(1)	0.1270(9)	1.021(2)	3.0(5)	C(29)	0.486(1)	0.085(1)	0.504(2)	2.3(4)
C(3)	0.788(1)	0.122(1)	1.067(2)	3.6(5)	C(30)	0.448(2)	0.043(1)	0.413(3)	4.7(6)
C(4)	0.843(1)	0.117(1)	0.973(2)	4.4(6)	C(31)	0.532(1)	0.010(1)	0.946(2)	3.5(5)
C(5)	0.824(1)	0.117(1)	0.845(2)	3.8(5)	C(32)	0.581(2)	−0.042(1)	0.968(3)	6.1(7)
C(6)	0.754(1)	0.1265(8)	0.806(2)	2.1(4)	C(33)	0.565(1)	0.246(1)	0.685(2)	3.3(5)
C(7)	0.924(1)	0.110(1)	1.017(2)	6.1(6)	C(34)	0.608(2)	0.306(1)	0.732(3)	5.8(7)
C(8)	0.738(1)	0.130(1)	0.673(2)	3.7(5)					

^{a} $B_{eq} = {}^8/_3\pi^2(U_{11}(aa^*)^2 + U_{22}(bb^*)^2 + U_{33}(bb^*)^2 + 2U_{12}aa^*bb^* \cos\gamma + 2U_{13}aa^*cc^* \cos\beta + 2U_{23}bb^*cc^* \cos\alpha)$.

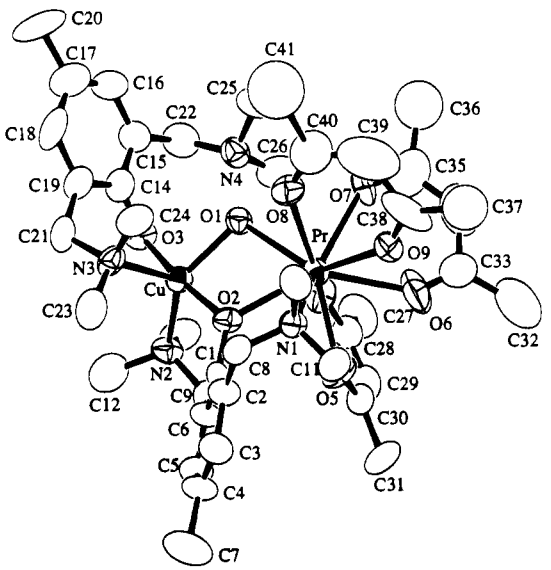

Figure 2. ORTEP diagram showing the molecular structure of **2** with labeling scheme and 50% thermal ellipsoids. Fluorine atoms are omitted for clarity.

Method B. Compound **3** can also be obtained in good yield from the direct reaction of **1** with $La(O_2CCF_3)_3$ by the same procedure as described for **2**.

Synthesis of $Cu_4(bdmmp)_2(\mu_4\text{-}O)(O_2CCF_3)_4$ (4). $Cu(OCH_3)_2$ (50 mg, 0.40 mmol) was added to a flask containing 10 mL of THF. 2,6-Bis[(dimethylamino)methyl]-4-methylphenol (89 mg, 0.40 mmol) was added to the solution. A brown solution was obtained. After the solution was stirred for 2 h at 23 °C, $Cu(O_2CCF_3)_2$ (116 mg, 0.40 mmol) and H_2O (4 mg, 0.20 mmol) were added. The solution color changed to olive green immediately. After being stirred for another 4 h, the solution was filtered and concentrated to about 5 mL *in vacuo*. Excess hexane was added to crystallize the product. After overnight standing at 23 °C, dark green crystals of **4** formed (110 mg, 0.095 mmol, 47% yield). The crystal of **4** decomposes at 275 °C. Anal. Calcd for $C_{34}H_{42}N_4O_{11}F_{12}Cu_4$: C, 35.06; H, 3.63; N, 4.81. Found: C, 35.27; H, 3.72; N, 4.84. IR (KBr, cm^{-1}): 1143 s, 1199 vs, 1260 m, 1343 w, 1434 w, 1478 m, 1631 w, 1683 s. UV–vis (1.0×10^{-4} M, THF; λ_{max}, nm): 214 (ϵ = 29 980 M^{-1} cm^{-1}), 242 (ϵ = 27 300 M^{-1} cm^{-1}), 283 (ϵ = 21 800 M^{-1} cm^{-1}), 645 (ϵ = 206 M^{-1} cm^{-1}, obtained from a 1.0×10^{-3} M solution).

X-ray Diffraction Analyses. Single crystals of **1**–**4** were grown from THF/hexane solutions and mounted on glass fibers with epoxy glue. Data was collected over the 2θ ranges 3–45° for **1** and 2–50° for **2**–**4** at 23 °C on a Rigaku AFC6-S diffractometer using graphite-monochromated Mo Kα radiation and operating at 50 kV and 35 mA. Three standard reflections were measured every 147 reflections. All data processing was performed on a Silicon Graphics computer using the TEXSAN crystallographic software package. All data were corrected for Lorentz–polarization effects and were not corrected for absorption due to the small absorption coefficients of the crystals.

The crystals of compound **1** were obtained in both nonsolvated and THF-solvated forms. The THF-solvated crystal of **1** has the empirical formula of $Cu(bdmmp)_2(H_2O)(THF)$ and belongs to the orthorhombic space group *Pbcn* (No. 60) (a = 16.552(4) Å, b = 9.865(3) Å, c = 20.301(4) Å), uniquely determined by the systematic absences ($0kl$, $k \neq 2n$; $h0l$, $l \neq 2n$; $hk0$, $h + k \neq 2n$). The nonsolvated crystal of **1** belongs to the monoclinic space group $C2/c$. The structure of **1** in both crystals is essentially identical (R = 0.060, R_w 0.049 for the THF solvated crystal). Therefore, only the details of the nonsolvated crystal structure are described here. Compound **2** crystallizes in the monoclinic space group $P2_1/n$ while compound **3** crystallizes in the triclinic space group $P\bar{1}$. Compound **4** belongs to the orthorhombic space group $P2_12_12_1$, uniquely determined by the systematic absences ($h00$, $h \neq 2n$; $0k0$, $k \neq 2n$; $00l$, $l \neq 2n$). The positions of metal atoms in all structures were determined by direct methods. All non-hydrogen atoms were located by subsequent difference Fourier syntheses. The hydrogen atoms on O(2) in **1** and on O(3) and N(1) in **3** were located directly from the difference Fourier maps. The positions of all other hydrogen atoms were calculated, and their contributions in structure factor calculations were included. The fluorine atoms bonded to C(32), C(36), C(37), and C(41) in **2** and the fluorine atoms bonded to C(28), C(30), and C(32) in **3** displayed a C_2 rotational disorder, which was successfully modeled. Two sets of fluorine atoms for each disordered CF_3 group were located and refined successfully with a 50% occupancy factor. A disordered hexane solvent molecule was located in the crystal lattice of **3** (one hexane/per molecule of **3**). The details of the crystallographic analysis are given in Table 1.

Results and Discussion

Synthesis and Structure of $Cu(bdmmp)_2(H_2O)$ (1). Compound **1** was obtained readily in good yield from the reaction

Table 3

(a) Selected Bond Lengths (Å) and Angles (deg) for **1**

Cu–O(1)	1.926(2)	O(1)–C(1)	1.357(4)	N(2)–C(12)	1.473(5)	C(6)–C(9)	1.485(6)
Cu–O(2)	2.055(4)	N(1)–C(8)	1.461(5)	N(2)–C(13)	1.459(5)	N(1)–C(10)	1.457(5)
Cu–N(2)	2.136(3)	N(1)–C(11)	1.469(5)	C(2)–C(8)	1.510(5)	N(2)–C(9)	1.481(5)
O(1)–Cu–O(1′)	176.3(2)	Cu–O(1)–C(1)	114.7(2)	C(9)–N(2)–C(13)	110.3(4)	C(3)–C(2)–C(8)	121.1(4)
O(1)–Cu–O(2)	88.1(1)	C(8)–N(1)–C(11)	110.4(4)	C(12)–N(2)–C(13)	108.4(3)	C(8)–N(1)–C(10)	111.4(3)
O(1)–Cu–N(2)	91.8(1)	C(1)–C(6)–C(9)	118.7(4)	O(1)–C(1)–C(2)	120.1(4)	C(10)–N(1)–C(11)	109.4(4)
O(1)–Cu–N(2′)	89.7(1)	N(1)–C(8)–C(2)	112.2(3)	O(1)–C(1)–C(6)	120.1(4)	C(5)–C(6)–C(9)	121.7(4)
O(2)–Cu–N(2)	114.50(9)	N(2)–C(9)–C(6)	113.2(4)	C(1)–C(2)–C(8)	120.3(4)	C(9)–N(2)–C(12)	110.0(3)
N(2)–Cu–N(2′)	131.0(2)						

(b) Selected Bond Lengths (Å) and Angles (deg) for **2**

Pr–O(1)	2.450(8)	C(2)–C(8)	1.50(2)	N(1)–C(8)	1.48(2)	N(4)–C(26)	1.49(2)
Pr–O(2)	2.424(8)	O(3)–C(14)	1.36(2)	N(1)–C(10)	1.48(2)	C(1)–C(6)	1.40(2)
Pr–O(4)	2.522(7)	C(6)–C(9)	1.49(2)	N(1)–C(11)	1.41(2)	O(2)–C(1)	1.37(2)
Pr–O(5)	2.481(9)	C(14)–C(15)	1.39(2)	N(2)–C(9)	1.52(2)	O(4)–C(28)	1.24(2)
Pr–O(6)	2.54(1)	C(14)–C(19)	1.39(2)	N(2)–C(12)	1.49(2)	O(5)–C(30)	1.21(2)
Pr–O(7)	2.52(1)	O(8)–C(40)	1.18(2)	N(2)–C(13)	1.45(2)	O(6)–C(33)	1.14(3)
Pr–O(8)	2.491(9)	C(19)–C(21)	1.50(2)	N(3)–C(21)	1.48(2)	O(7)–C(35)	1.16(3)
Pr–O(9)	2.46(1)	C(38)–C(39)	1.57(4)	N(3)–C(23)	1.43(2)	C(15)–C(22)	1.48(2)
Cu–O(1)	2.033(8)	C(39)–C(40)	1.47(4)	N(3)–C(24)	1.47(2)	C(28)–C(29)	1.38(2)
Cu–O(2)	1.958(8)	C(34)–C(35)	1.49(4)	N(4)–C(22)	1.49(2)	C(29)–C(30)	1.40(2)
Cu–O(3)	1.915(8)	O(9)–C(38)	1.11(2)	N(4)–C(25)	1.47(2)	C(33)–C(34)	1.48(4)
Cu–N(2)	2.10(1)						
Cu–N(3)	2.30(1)						
C(1)–C(2)	1.39(2)						
O(1)–Pr–O(2)	64.3(3)	O(4)–Pr–O(5)	68.8(3)	O(7)–Pr–O(9)	73.5(3)	Pr–O(2)–Cu	107.2(3)
O(1)–Pr–O(4)	74.8(3)	O(4)–Pr–O(6)	68.3(3)	O(8)–Pr–O(9)	68.6(3)	O(4)–Pr–O(7)	79.4(3)
O(1)–Pr–O(5)	126.5(3)	O(4)–Pr–O(8)	136.7(3)	O(1)–Cu–O(2)	81.0(3)	O(4)–Pr–O(9)	131.6(3)
O(1)–Pr–O(6)	132.8(3)	O(5)–Pr–O(6)	64.6(4)	O(1)–Cu–O(3)	92.0(3)	O(5)–Pr–O(7)	129.8(3)
O(1)–Pr–O(7)	77.3(3)	O(5)–Pr–O(8)	153.9(3)	O(1)–Cu–N(2)	136.5(4)	O(5)–Pr–O(9)	99.5(3)
O(1)–Pr–O(8)	68.6(3)	O(6)–Pr–O(7)	68.0(4)	O(1)–Cu–N(3)	106.1(3)	O(6)–Pr–O(8)	124.0(4)
O(1)–Pr–O(9)	134.0(3)	C(8)–N(1)–C(10)	105.4(9)	O(2)–Cu–O(3)	172.1(4)	O(6)–Pr–O(9)	64.6(3)
O(2)–Pr–O(4)	85.6(2)	C(8)–N(1)–C(11)	110(1)	O(2)–Cu–N(2)	93.5(4)	O(7)–Pr–O(8)	70.8(3)
O(2)–Pr–O(5)	74.9(3)	C(10)–N(1)–C(11)	106(1)	O(2)–Cu–N(3)	94.0(3)	C(9)–N(2)–C(12)	109(1)
O(2)–Pr–O(6)	137.4(3)	C(9)–N(2)–C(13)	105(1)	O(3)–Cu–N(2)	89.0(4)	C(12)–N(2)–C(13)	109(1)
O(2)–Pr–O(7)	141.3(3)	C(21)–N(3)–C(23)	110(1)	O(3)–Cu–N(3)	91.5(4)	C(21)–N(3)–C(24)	108(1)
O(2)–Pr–O(8)	98.3(3)	C(23)–N(3)–C(24)	110(1)	N(2)–Cu–N(3)	117.4(4)	C(22)–N(4)–C(25)	111(1)
O(2)–Pr–O(9)	138.5(3)	C(22)–N(4)–C(26)	112(1)	Pr–O(1)–Cu	103.9(3)	C(25)–N(4)–C(26)	109(1)

(c) Selected Bond Lengths (Å) and Angles (deg) for **3**

La–O(1)	2.432(8)	N(1)–C(1)	1.55(2)	La–O(3)	2.471(8)	O(9)–C(31)	1.24(2)
La–O(4)	2.412(9)	N(1)–C(11)	1.48(2)	La–O(6)	2.58(1)	N(1)–C(10)	1.45(2)
La–O(7′)	2.504(9)	N(2)–C(9)	1.49(2)	La–O(8)	2.529(9)	C(20)–C(21)	1.41(2)
La–O(9′)	2.563(9)	N(2)–C(12)	1.45(2)	La–N(3)	2.90(1)	C(20)–C(22)	1.45(2)
Cu–O(1)	1.963(8)	N(3)–C(14)	1.49(2)	Cu–O(2)	1.900(8)	N(2)–C(13)	1.47(2)
Cu–O(3)	2.098(8)	N(3)–C(24)	1.46(2)	Cu–N(2)	2.30(1)	N(3)–C(23)	1.49(2)
Cu–N(4)	2.10(1)	N(4)–C(25)	1.46(2)	O(1)–C(21)	1.35(1)	N(4)–C(22)	1.51(2)
O(2)–C(8)	1.32(2)	C(1)–C(2)	1.49(2)	O(4)–C(27)	1.20(2)	N(4)–C(26)	1.47(2)
O(5)–C(27)	1.24(2)	C(7)–C(8)	1.40(2)	O(6)–C(29)	1.20(2)	C(2)–C(8)	1.44(2)
O(7)–C(29)	1.27(2)	C(14)–C(15)	1.49(2)	C(15)–C(21)	1.38(2)	C(17)–C(9)	1.49(2)
O(8)–C(31)	1.25(2)						
O(1)–La–O(3)	65.9(3)	O(6)–La–O(7′)	115.4(3)	O(9′)–La–N(3)	141.8(3)	O(4)–La–N(3)	76.5(3)
O(1)–La–O(4)	103.0(3)	O(6)–La–O(9′)	76.4(3)	O(1)–Cu–O(2)	172.3(4)	O(6)–La–O(8)	68.6(3)
O(1)–La–O(6)	82.6(3)	O(7′)–La–O(8)	75.6(3)	O(1)–Cu–O(3)	82.0(3)	O(6)–La–N(3)	138.2(3)
O(1)–La–O(7′)	141.8(3)	O(7′)–La–N(3)	75.1(3)	O(1)–Cu–N(2)	97.1(4)	O(7′)–La–O(9′)	73.8(3)
O(1)–La–O(8)	81.3(3)	La–O(1)–Cu	107.6(4)	O(1)–Cu–N(4)	91.3(4)	O(8)–La–O(9′)	116.2(3)
O(1)–La–O(9′)	144.3(3)	C(1)–N(1)–C(10)	110(1)	O(2)–Cu–O(3)	92.1(4)	La–O(3)–Cu	101.9(3)
O(1)–La–N(3)	70.1(3)	C(10)–N(1)–C(11)	110(1)	O(2)–Cu–N(2)	89.2(4)	C(1)–N(1)–C(11)	112(1)
O(3)–La–O(4)	75.9(3)	C(12)–N(2)–C(13)	108(1)	O(2)–Cu–N(4)	89.7(4)	C(9)–C(2)–C(13)	107(1)
O(3)–La–O(6)	72.6(3)	C(14)–N(3)–C(24)	108(1)	O(3)–Cu–N(2)	104.4(4)	C(14)–N(3)–C(23)	106(1)
O(3)–La–O(7′)	149.6(3)	C(22)–N(4)–C(25)	109(1)	O(3)–Cu–N(4)	137.7(4)	C(23)–N(3)–C(24)	108(1)
O(3)–La–O(8)	131.6(3)	C(25)–N(4)–C(26)	106(1)	N(2)–Cu–N(4)	117.9(4)	C(22)–N(4)–C(26)	108(1)
O(3)–La–O(9′)	80.3(3)	O(8)–C(31)–O(9)	131(1)	O(4)–La–O(6)	142.2(3)	O(4)–C(2)–O(5)	133(2)
O(3)–La–N(3)	119.9(3)	O(8)–La–N(3)	76.3(3)	O(4)–La–O(8)	149.0(3)	O(6)–C(9)–O(7)	128(2)
O(4)–La–O(7′)	83.3(3)						
O(4)–La–O(9′)	78.2(3)						

(d) Selected Bond Lengths (Å) and Angles (deg) for **4**

Cu(1)–O(1)	1.97(1)	Cu(4)–N(3)	2.01(2)	Cu(1)–O(2)	1.90(1)	N(1)–C(10)	1.43(3)
Cu(1)–O(6)	1.94(1)	O(2)–C(1)	1.40(2)	Cu(1)–O(9)	2.58(1)	N(2)–C(11)	1.52(2)
Cu(1)–N(1)	2.05(2)	O(4)–C(27)	1.27(3)	Cu(2)–O(1)	1.88(1)	O(3)–C(14)	1.40(2)
Cu(2)–O(2)	1.96(1)	O(6)–C(29)	1.23(2)	Cu(2)–O(4)	1.98(2)	O(5)–C(27)	1.20(3)

Table 3 (Continued)

Cu(2)–O(11)	2.48(2)	N(2)–C(12)	1.44(3)	Cu(2)–N(2)	2.04(1)	O(7)–C(29)	1.25(3)
Cu(3)–O(1)	1.93(1)	N(3)–C(21)	1.58(3)	Cu(3)–O(3)	1.96(1)	N(2)–C(13)	1.49(3)
Cu(3)–O(7)	2.42(1)	N(3)–C(23)	1.44(3)	O(8)–C(33)	1.26(3)	N(3)–C(22)	1.45(3)
Cu(3)–O(8)	1.95(1)	N(4)–C(25)	1.42(3)	O(9)–C(33)	1.16(3)	N(4)–C(24)	1.44(2)
Cu(3)–N(4)	1.98(2)	C(1)–C(2)	1.33(3)	O(10)–C(31)	1.21(3)	N(4)–C(26)	1.56(3)
Cu(4)–O(1)	1.94(1)	C(2)–C(11)	1.57(3)	O(11)–C(31)	1.22(3)	C(1)–C(6)	1.41(3)
Cu(4)–O(3)	1.91(1)	C(14)–C(19)	1.45(3)	N(1)–C(8)	1.57(3)	C(14)–C(15)	1.36(3)
Cu(4)–O(5)	2.40(2)	C(19)–C(21)	1.47(3)	N(1)–C(9)	1.37(3)	C(15)–C(24)	1.52(3)
Cu(4)–O(10)	1.96(1)						
O(2)–Cu(2)–N(2)	92.1(5)	O(1)–Cu(4)–O(10)	94.4(5)	O(4)–Cu(2)–O(11)	112.5(6)	O(1)–Cu(4)–N(3)	174.3(6)
O(4)–Cu(2)–N(2)	91.1(6)	O(3)–Cu(4)–O(5)	94.5(5)	O(11)–Cu(2)–N(2)	90.5(6)	O(3)–Cu(4)–O(10)	156.4(6)
O(1)–Cu(1)–O(2)	80.8(5)	O(3)–Cu(4)–N(3)	93.6(6)	O(1)–Cu(1)–O(6)	94.4(5)	O(5)–Cu(4)–O(10)	108.9(6)
O(1)–Cu(1)–O(9)	93.0(5)	O(5)–Cu(4)–N(3)	86.1(6)	O(1)–Cu(1)–N(1)	174.2(6)	C(8)–N(1)–C(10)	107(2)
O(2)–Cu(1)–O(6)	163.1(6)	O(10)–Cu(4)–N(3)	91.0(6)	O(1)–Cu(3)–O(3)	80.9(5)	C(9)–N(1)–C(10)	114(2)
O(2)–Cu(1)–O(9)	86.1(5)	Cu(1)–O(1)–Cu(2)	99.1(5)	O(1)–Cu(3)–O(7)	93.7(5)	C(8)–N(1)–C(9)	107(2)
O(2)–Cu(1)–N(1)	93.6(6)	Cu(1)–O(1)–Cu(3)	108.0(6)	O(1)–Cu(3)–O(8)	93.5(5)	C(11)–N(2)–C(12)	118(1)
O(6)–Cu(1)–O(9)	110.4(5)	Cu(1)–O(1)–Cu(4)	119.7(6)	O(1)–Cu(3)–N(4)	173.7(6)	C(11)–N(2)–C(13)	104(2)
O(6)–Cu(1)–N(1)	90.6(6)	Cu(2)–O(1)–Cu(3)	120.1(6)	O(3)–Cu(3)–O(7)	87.9(5)	C(12)–N(2)–C(13)	111(2)
O(9)–Cu(1)–N(1)	87.9(6)	Cu(2)–O(1)–Cu(4)	112.8(6)	O(3)–Cu(3)–O(8)	161.8(5)	C(21)–N(3)–C(22)	108(2)
O(3)–Cu(3)–N(4)	92.8(6)	Cu(3)–O(1)–Cu(4)	98.4(5)	O(7)–Cu(3)–O(8)	109.8(5)	C(21)–N(3)–C(23)	107(2)
O(7)–Cu(3)–N(4)	86.5(6)	Cu(1)–O(2)–Cu(2)	98.7(6)	O(8)–Cu(3)–N(4)	92.3(6)	C(22)–N(3)–C(23)	107(2)
O(1)–Cu(2)–O(2)	81.4(5)	Cu(3)–O(3)–Cu(4)	98.6(5)	O(1)–Cu(2)–O(4)	94.6(5)	C(24)–N(4)–C(25)	110(2)
O(1)–Cu(2)–O(11)	90.4(5)	C(24)–N(4)–C(26)	102(1)	O(1)–Cu(2)–N(2)	173.4(5)	C(25)–N(4)–C(26)	107(2)
O(2)–Cu(2)–O(4)	159.2(6)	O(4)–C(27)–O(5)	131(2)	O(1)–Cu(4)–O(3)	82.0(5)	O(6)–C(29)–O(7)	126(2)
O(2)–Cu(2)–O(11)	87.9(5)	O(10)–C(31)–O(11)	134(2)	O(1)–Cu(4)–O(5)	90.6(5)	O(8)–C(33)–O(9)	136(2)

of $Cu(OCH_3)_2$ with bdmmpH in THF. Elemental and X-ray diffraction analyses established its formula as $Cu(bdmmp)_2(H_2O)$. The H_2O ligand is believed to come from the highly hygroscopic bdmmpH reagent. The structure of **1** was determined by single-crystal X-ray diffraction analysis. Positional and thermal parameters are given in Table 2a. Selected bond lengths and angles are listed in Table 3a. As shown in Figure 1, compound **1** possesses a C_2 axis on which the Cu and O(2) atoms lie. The copper center has a trigonal bipyramidal geometry with O(1) and O(1′) occupying the axial positions and O(2), N(2), and N(2′) occupying the equatorial positions. All copper–ligand bond distances are within the range of normal bond lengths while the angles on the equatorial plane (O(2)–Cu–N(2) = 114.50(9)°, N(2)–Cu–N(2′) = 131.0(2)°) are somewhat deviated from an ideal trigonal plane. A similar situation has been observed previously in the compound[5] $[Cu(bipy)_2(H_2O)](S_2O_6)$. Copper(II) complexes with alkoxo ligands are usually dinuclear or polynuclear due to the tendency of the alkoxo ligand to function as a bridging ligand. In fact, mononuclear copper(II) complexes with alkoxo ligands are rare.[6] The coordination saturation and the steric effect of the dangling amino groups in **1** may contribute to its stability. The other interesting feature in **1** is the formation of two hydrogen bonds between the H_2O ligand and the two dangling dimethylamino groups, as shown by the O(2)–N(1) distance of 2.756(4) Å. Although the position of the hydrogen atom cannot be accurately determined by X-ray diffraction analysis, the approximate location of H(22) was established from the crystallographic data, which show unambiguously that the hydrogen atom is bonded to the O(2) atom (O(2)–H(22) = 1.05 Å). Due to the crystallographically imposed C_2 symmetry, the H_2O ligand has an unusual trigonal planar geometry, in contrast to the typical pyramidal geometry. The planar geometry of the H_2O ligand could also be the result of the formation of hydrogen bonds with the two amino groups. In fact, it has been observed previously that hydrogen bonds could lead to a planar geometry of the H_2O molecule.[7] The Cu–O(2) distance of 2.055(4) Å is significantly shorter than the previously reported Cu(II)–OH_2 distances in a similar trigonal bipyramidal environment,[6] which are typically longer than 2.15 Å. We believe that the formation of two hydrogen bonds with the amino groups enhances the nucleophilicity of the O(2) atom, resulting in the relative short Cu–O(2) bond. The nucleophilicity of this coordinated H_2O ligand is further demonstrated by the facile formation of heteronuclear Ln–Cu complexes via the reactions of **1** with $Ln(O_2CCF_3)_3$ or $Ln(hfacac)_3$, where the H_2O ligand was transformed to an OH ligand, bridging a Cu(II) and a Ln(III) ion (Scheme 1).

Synthesis and Structure of $Pr^{III}Cu^{II}$(bdmmpH)(bdmmp)(μ-OH)(hfacac)$_3$ (2). Compound **2** can be obtained readily in good yield from the reaction of $Cu(OCH_3)_2$ with bdmmpH and $Pr(hfacac)_3$ in a 1:2:1 ratio where the mononuclear compound **1** is believed to be the precursor. Indeed, compound **2** can also be obtained from the direct reaction of $Cu(bdmmp)_2(H_2O)$ with $Pr(hfacac)_3$ in a 1:1 ratio. Compound **2** is stable in the solid state but undergoes slow decomposition in solution upon exposure to air. This dark green compound has been fully characterized by X-ray diffraction and elemental analyses and formulated as $PrCu(bdmmpH)(bdmmp)(\mu\text{-}OH)(hfacac)_3$. Important positional and thermal parameters are given in Table 2b. Selected bond lengths and angles are listed in Table 3b. Compound **2** is a dinuclear complex where the $Pr(hfacac)_3$ unit is linked to the copper monomer through a hydroxo and a phenoxo bridge with a Pr–Cu distance of 3.538(2) Å, as shown in Figure 2. The copper(II) center has a trigonal bipyramidal geometry similar to that of **1** with O(2) and O(3) occupying the axial positions (O(2)–Cu–O(3) = 172.1(4)°) and O(1), N(2), and N(3) occupying the equatorial positions. However, the O(1)–Cu–N(2), O(1)–Cu–N(3), and N(2)–Cu–N(3) angles of 136.5(4), 106.1(3), and 117.4(4)° are further deviated from the ideal trigonal plane than those in **1**, and the Cu–N(3) distance of 2.30(1) Å is much longer than those in **1**, implying an increased degree of distortion toward a square pyramidal geometry. The Pr(III) ion is surrounded by one nitrogen and

(5) Harrison, W. D.; Hathaway, B. J. *Acta Crystallogr., Sect. B* **1979**, *35*, 2910.

(6) Hathaway, B. J. In *Comprehensive Coordination Chemistry*; Wilkinson, G., Gillard, R. D., McCleverty, J. A., Eds.; Pergamon Press: Oxford, U.K., 1987; Vol. V, Chapter 53 and references therein.

(7) (a) Emsley, J. *Chem. Soc. Rev.* **1980**, *9*, 91. (b) *The Hydrogen Bond*; Schuster, P., Zundel, G., Sandorfy, C., Eds.; North-Holland Publishing Co.: Amsterdam, 1976; Vol. II.

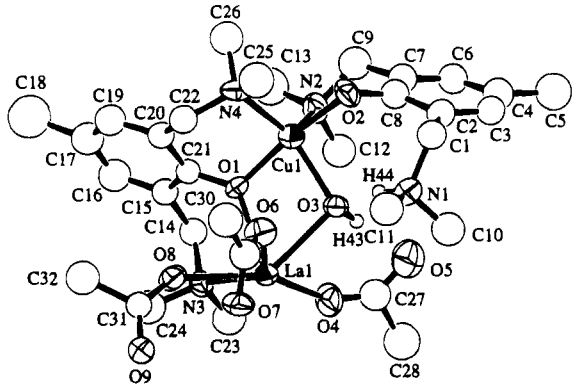

Figure 3. ORTEP diagram showing the dinuclear unit of compound **3** with labeling scheme and 50% thermal ellipsoids. Fluorine atoms are omitted for clarity.

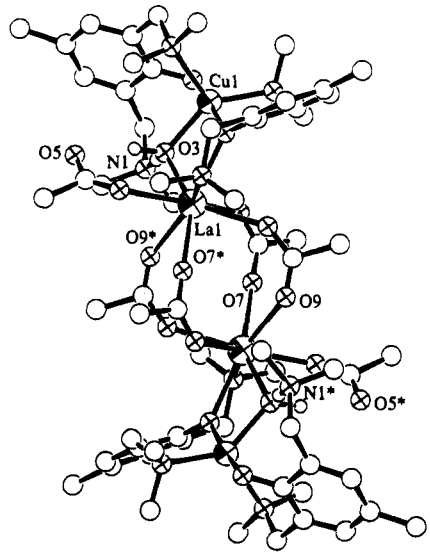

Figure 4. Diagram showing the dimeric structure of **3**. All atoms are shown as ideal spheres, and fluorine atoms are omitted for clarity.

eight oxygen atoms in an irregular polyhedral geometry. While the Pr–O bond distances range from 2.424(8) to 2.54(1) Å, the Pr–N(1) distance of 2.90(1) Å is much longer. The poor affinity of the amino group for the lanthanide(III) center, in comparison with the negatively charged oxygen atoms, has also been observed previously in Ln–Cu complexes with the 1,3-bis(dimethylamino)-2-propanolato ligand.[3] The OH ligand is believed to come from the H_2O ligand in **1**. Although the acidic proton in **2** could not be located in the X-ray diffraction analysis, we believe that it is bonded to the N(4) atom and hydrogen-bonded to the O(1) atom, as supported by the N(4)–O(1) distance of 2.69(1) Å and the structure of **3** (see also the discussion on compound **3**). The OH group also appears to form a hydrogen bond with the O(8) atom of a hfacac ligand, as evidenced by the O(1)–O(8) distance of 2.78(1) Å. The transformation of the H_2O ligand to the OH ligand was apparently facilitated by the presence of the uncoordinated amino group, functioning as a Lewis base, and hydrogen-bonding interactions. In addition, the lanthanide(III) ions could also promote the formation of the hydroxo ligand due to their high affinity for the oxygen atom.[8] Several heteronuclear Ln–Cu complexes are known;[1] however, compound **2** is among the few examples of Ln–Cu complexes with a discrete dinuclear structure in the solid state.[2]

Synthesis and Structure of $[La^{III}Cu^{II}(bdmmpH)(bdmmp)(\mu\text{-}OH)(O_2CCF_3)_3]_2$ (3). Compound **3** was obtained in good yield in the same manner as that for the synthesis of **2**, via either the reaction of $Cu(OCH_3)_2$ with bdmmpH and $La(O_2CCF_3)_3$ in a 1:2:1 ratio or the reaction of compound **1** with 1 equiv of $La(O_2CCF_3)_3$. This dark green compound decomposes slowly in solution upon exposure to air but is stable in the solid state. Elemental and X-ray diffraction analyses established the formula of **3** as $[LaCu(bdmmpH)(bdmmp)(\mu\text{-}OH)(O_2CCF_3)_3]_2$. Selected positional and thermal parameters are given in Table 2c, and important bond lengths and angles are listed in Table 3c. As shown in Figures 3 and 4, compound **3** consists of two dinuclear units of $LaCu(bdmmpH)(bdmmp)(\mu\text{-}OH)(O_2CCF_3)_3$, related by an inversion center symmetry operation. The structure of the dinuclear unit resembles that of compound **2**, where the $La(O_2CCF_3)_3$ unit is linked to the copper(II) monomer via a hydroxo and a phenoxo bridge with a La–Cu distance of 3.556(2) Å. The Cu(II) center again has a distorted trigonal bipyramidal geometry with the O(1) and O(2) atoms occupying the axial positions (O(1)–Cu–O(2) = 172.3(4)°) and O(3), N(2), and N(4) on the equatorial plane (O(3)–Cu–N(2) = 104.4(4)°, O(3)–Cu–N(4) = 137.7(4)°, N(2)–Cu–N(4) = 117.9(4)°). The approximate positions of the protons bonded to O(3) and N(1) were determined by the X-ray diffraction analysis, which unambiguously established that the acidic proton H(44) is bonded to the N(1) amino group and hydrogen-bonded to the OH ligand (N(1)–O(3) = 2.64(1) Å), as occurred in compound **2**. The proton H(43) of the OH ligand is believed to form a hydrogen bond with the uncoordinated O(5) of a trifluoroacetate ligand, as evidenced by the O(3)–O(5) distance of 2.96(1) Å. The hydrogen-bonding pattern in **3** is therefore similar to that in **2**. Most interestingly, instead of functioning as a chelating ligand, four of the trifluoroacetate ligands in **3** act as bridging ligands to link the two dinuclear LaCu units. As a result, the La(III) center is surrounded by seven oxygen atoms, with bond lengths ranging from 2.412(9) to 2.58(1) Å, and a weakly bonded nitrogen atom (La–N(3) = 2.90(1) Å). A similar bonding situation has been observed in the complex $[SrCu(bdmap)_2(O_2CCF_3)_2]_2$, bdmap = 1,3-bis(dimethylamino)-2-propanolato, where the trifluoroacetate ligands link two SrCu units.[9] The structural difference between compounds **2** and **3** is clearly caused by the tendency of the hfacac ligand in **2** to chelate and the tendency of the carboxylate ligand in **3** to bridge.

The syntheses of compounds **2** and **3** demonstrate the utility of the mononuclear copper(II) compound **1** as a precursor for the formation of heteronuclear complexes involving highly electropositive elements such as lanthanides. Compound **1** has also been found to be useful for the synthesis of Bi(III)–Cu(II) complexes. Unfortunately the structural characterization of the Bi(III)–Cu(II) complex was unsuccessful due to the lack of suitable single crystals for X-ray diffraction analysis.

Synthesis and Structure of $Cu_4(bdmmp)_2(\mu_4\text{-}O)(O_2CCF_3)_4$ (4). Compound **4**, isolated initially from an attempted reaction for the synthesis of Bi–Cu complexes, can be synthesized in good yield by the reaction of $Cu(OCH_3)_2$, bdmmpH, $Cu(O_2CCF_3)_2$, and H_2O in a 1:1:1:0.5 ratio in THF. Elemental and X-ray diffraction analyses established the formula of **4** as $Cu_4(bdmmp)_2(\mu_4\text{-}O)(O_2CCF_3)_4$. Important positional and thermal parameters are given in Table 2d, and Selected bond lengths and angles are listed in Table 3d. The molecular structure of **4** is shown in Figure 5. Compound **4** consists of four Cu(II) ions bridged by an oxygen atom in an approximately tetrahedral environment. The oxygen atom of the bdmmp ligand bridges

(8) Hart, F. A. In *Comprehensive Coordination Chemistry*; Wilkinson, G., Gilard, R. D., McCleverty, J. A., Eds.; Pergamon Press: New York, 1987; Vol. III, Chapter 39 and references therein.

(9) Breeze, S. R.; Wang, S. *Inorg. Chem.* **1994**, *33*, 5113.

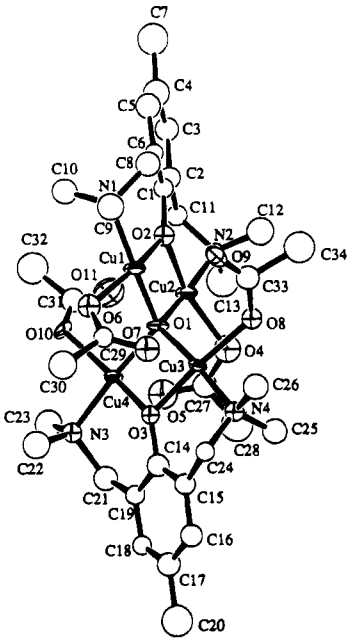

Figure 5. ORTEP diagram showing the molecular structure of **4** with labeling scheme and 50% thermal ellipsoids. Fluorine atoms are omitted for clarity.

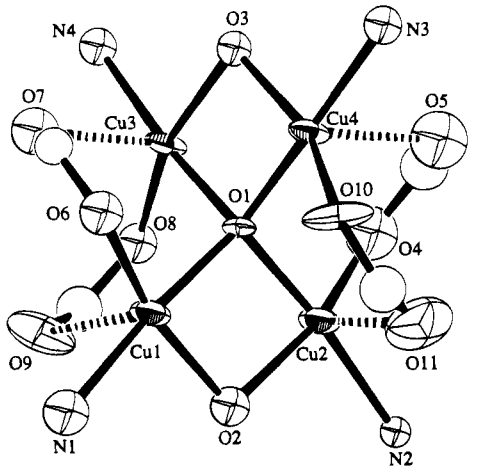

Figure 6. ORTEP diagram showing the core structure of **4**.

two copper centers, resulting in the Cu(1)–Cu(2) and Cu(3)–Cu(4) distances of 2.930(3) and 2.933(3) Å, the shortest among the six Cu–vectors in **4**. Each copper center is coordinated by three oxygen atoms and one nitrogen atom, with the bond lengths ranging from 1.90(1) to 2.05(2) Å. There are considerable deviations of the geometry of the copper center from the ideal square plane, as indicated by the basal plane angles (Table 3c), although each CuO_3N portion is essentially planar. The dihedral angles between the Cu(1) and Cu(2) planes and between the Cu(3) and Cu(4) planes are 11.2 and 13.6°, respectively. The two $Cu_2O_4N_2$ dinuclear units are nearly perpendicular as evidenced by the dihedral angle of 97.5° between the Cu(1)O(1)Cu(2)O(2) and Cu(3)O(1)Cu(4)O(3) planes. The fifth position of each copper center is occupied by an oxygen atom of the trifluoroacetate ligand, with the Cu–O bond lengths ranging from 2.40(2) to 2.58(1) Å (Figure 6). The geometry of the copper center therefore can be best described as a distorted square pyramid. As shown in Figure 6, the pattern of the trifluoroacetate bridges in **4** is rather symmetric: two of them link Cu(1) and Cu(3), and the other two link Cu(2) and Cu(4). Perhaps as a consequence, the Cu(1)–Cu(3) and Cu(2)–Cu(4) distances of 3.155(3) and 3.184(3) Å are substantially shorter

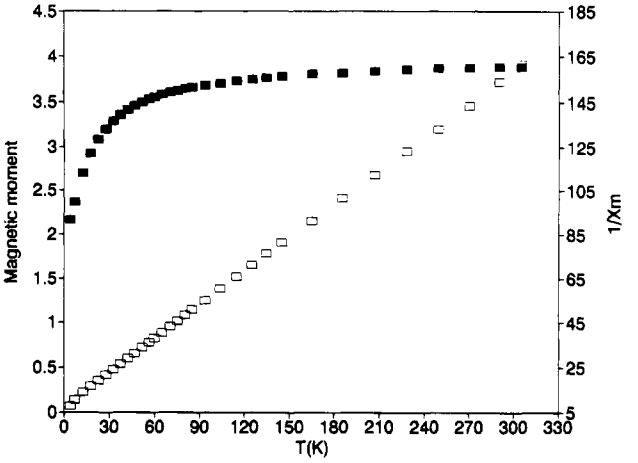

Figure 7. Plots of χ_M^{-1} (empty square) and magnetic moment (filled square) of **2** vs temperature (K).

than those of Cu(1)–Cu(4) and Cu(2)–Cu(3) (3.379(3) and 3.306(3) Å). Examples of tetranuclear copper(II) complexes with a μ_4-O kernel are abundant, but most of them involve halogen ligands.[10] Krebs and co-workers recently reported a Cu_4 complex of the formula $[Cu_4(\mu_4\text{-}O)(OBz)_4(bmmk)_2](H_2O)$, OBz = benzoate, bmmk = 2,6-bis(morpholinomethyl)-4-methylphenolato, where the four copper atoms have an arrangement similar to that observed in **4**, but the pattern of the benzoate bridges is not symmetric due to the presence of a H_2O ligand.[10d]

Magnetic Properties. The magnetic susceptibilities of **2** and **4** were measured over the temperature range 4–310 K. The reciprocal molar susceptibility (χ^{-1}) and magnetic moment of **2** versus temperature (K) are shown in Figure 7. Compound **2** has a magnetic moment of 3.88 μ_B at 305 K, which is slightly smaller than the value of 4.05 μ_B, assuming both Pr(III) and Cu(II) as noninteracting ions with magnetic moments of 3.58 and 1.90 μ_B, respectively. The magnetic moment of **2** is nearly constant at temperatures above 200 K. The decrease of magnetic moment at low temperature implies the presence of some degree of antiferromagnetic exchange. The χ^{-1} curve is almost a straight line with a small deviation at low temperature, suggesting that the magnetic exchange constant must be small. In fact, it has been frequently observed before that the magnetic exchange between Cu(II) and Ln(III) is often associated with a J value in the range of 0 to ± 10 cm^{-1}, perhaps attributable to the ineffective overlaps of the f orbitals of the Ln(III) ion with the orbitals on the bridging ligand.[1c,1i]

The μ_{eff} of compound **4** at 290 K is 1.41 μ_B per copper, much smaller than that of a noninteracting Cu(II) ion ($\mu \approx 1.7$–1.9 μ_B), implying the presence of magnetic exchange. As shown in Figure 8, the magnetic susceptibility of **4** has a minimum at 32 K and a maximum at 185 K. The rise of the susceptibility at low temperature is due to the presence of paramagnetic impurities. The susceptibility data were corrected for diamagnetism (Pascal corrections) and further corrected for temperature-independent paramagnetism (TIP) and the presence of paramagnetic monomer impurity according to (1).

The data were fit initially by using the Bleaney–Bowers equation which produced $J = -101$ cm^{-1}, $g = 1.86$, $\varrho = 0.0065$, $\chi_{TIP} = 4.8 \times 10^{-5}$, and $R = \sum[(\chi_{calc} - \chi_{exp})/\chi_{exp}]^2 = 2.05\%$. The reasonable fit of the data to the simple dimer model

(10) (a) Davis, G.; El-Shazly, M. F.; Rupich, M. W.; Churchill, M. R.; Rotella, F. J. *J. Chem. Soc., Chem. Commun.* **1978**, 1045. (b) Churchill, M. R.; Rotella, F. J. *Inorg. Chem.* **1979**, *18*, 853. (c) Cai, C.-Z.; Davies, G.; El-Toukhy, A.; Gilbert, T. R.; Henany, M. *Inorg. Chem.* **1985**, *24*, 1701. (d) Teipel, S.; Griesar, K.; Hasse, W.; Krebs, B. *Inorg. Chem.* **1994**, *33*, 456.

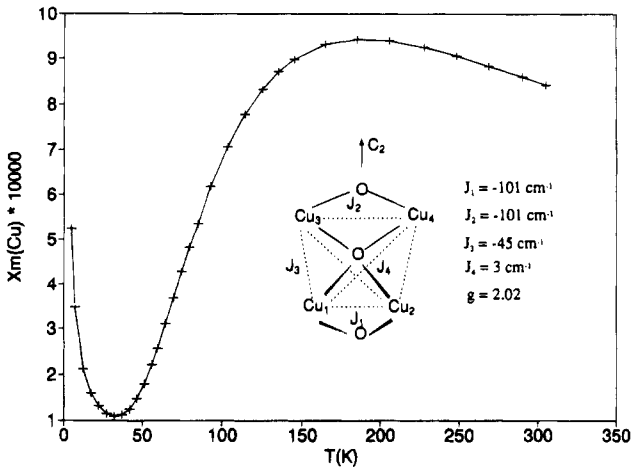

Figure 8. Plot of χ_m of **4** vs temperature (K). The solid line is the fitting.

$$\chi_{calc} = (1 - \varrho)\chi + \chi_{TIP} + \varrho\chi_{mono} \quad (1)$$

ϱ = fraction of paramagnetic impurity

χ_{TIP} = temperature-independent paramagnetism

χ_{mono} = magnetic susceptibility from the monomer impurity

implies that the spin exchange in compound **4** is dominated by antiferromagnetism within the $Cu_2O_4N_2$ dimer. The low g value from the dimer fitting, however, suggests that a better fitting model should be used. We therefore fitted the data by using the tetramer model **A**. Due to the C_2 symmetry of the tetramer,

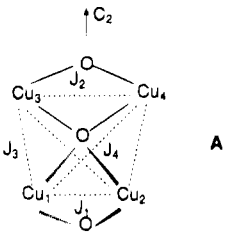

A

the spin-exchange Hamiltonian can be reduced to eq 2, where

$$\hat{H} = 2(J_1\hat{S}_1\hat{S}_2 + J_2\hat{S}_3\hat{S}_4 + 2J_3\hat{S}_1\hat{S}_3 + 2J_4\hat{S}_1\hat{S}_4) \quad (2)$$

$J_1 = J_{1-2}$, $J_2 = J_{3-4}$, $J_3 = J_{1-3} = J_{2-4}$, and $J_4 = J_{2-3} = J_{1-4}$. The general susceptibility expression (eq 3), as derived[11] from

$$\chi = \frac{2Ng^2\beta^2}{kT} \times \frac{5e^{-E_q/kT} + e^{-E_{T1}/kT} + e^{-E_{T2}/kT} + e^{-E_{T3}/kT}}{5e^{-E_q/kT} + 3e^{-E_{T1}/kT} + 3e^{-E_{T2}/kT} + 3e^{-E_{T3}/kT} + e^{-E_{S1}/kT} + e^{-E_{S2}/kT}} \quad (3)$$

the general van Vleck equation, was used for fitting experimental χ data by using a nonlinear regression program where $E_q = -(J_1 + J_2 + 2J_3 + 2J_4)/2$, $E_{T1} = -(J_1 + J_2 - 2J_3 - 2J_4)/2$, $E_{T2} = -(J_1 + J_2 + 2((J_1 - J_2)^2 + (J_3 - J_4)^2)^{1/2})/2$, $E_{T3} = -(J_1 + J_2 - 2((J_1 - J_2)^2 + (J_3 - J_4)^2)^{1/2})$, $E_{S1} = (J_1 + J_2 + 2J_3 + 2J_4 + 2((J_1 + J_2 - J_3 - J_4)^2 + 3(J_2 - J_3)^2)^{1/2}/2$, and $E_{S2} = (J_1 + J_2 + 2J_3 + 2J_4 - 2((J_1 + J_2 - J_3 - J_4)^2 + 3(J_3 - J_4)^2)^{1/2})/2$.

(11) (a) Sinn, E. *Coord. Chem. Rev.* **1970**, *5*, 313. (b) Hall, J. W.; Estes, E. D.; Scaringe, R. P.; Hatfield, W. E. *Inorg. Chem.* **1977**, *16*, 1572.

The fitting results are shown in Figure 8. The best fit of the data gave $J_1 = -101$ cm^{-1}, $J_2 = -101$ cm^{-1}, $J_3 = -45$ cm^{-1}, $J_4 = 3$ cm^{-1}, $g = 2.02$, $\varrho = 0.024$, $\chi_{TIP} = 1.2 \times 10^{-4}$, and $R = \sum[(\chi_{calc} - \chi_{exp})/\chi_{exp}]^2 = 0.68\%$. The R and g value from the tetramer fitting are substantially improved in comparison with the dimer fitting results. The tetramer fitting results indicate that the magnetism in compound **4** is dominated by the antiferromagnetic exchange within the dimers of Cu(1)−Cu(2) and Cu(3)−Cu(4); the interdimer interactions, albeit weaker, are substantial. The exchange constant J_3 was assigned to the two shorter vectors Cu(1)−Cu(3) (3.155(3) Å) and Cu(2)−Cu(4) (3.184(3) Å) where the two copper atoms are bridged by the oxo and two acetate ligands, while J_4 was assigned to the two longer vectors Cu(2)−Cu(3) (3.306(3) Å) and Cu(1)−Cu(4) (3.379(3) Å) where the two copper atoms are bridged by the oxo ligand only. These assignments are tentative due to the complexity of the system. A detailed theoretical investigation is necessary in order to fully understand the nature of the magnetic exchanges in this system.

One interesting observation is that although compound **4** clearly does not belong to the class of dinuclear Cu(II) complexes with bis(μ-hydroxo) bridges, the exchange constants J_1 and J_2 within the Cu(1)−Cu(2) and Cu(3)−Cu(4) dinuclear units are in agreement with the values predicted by an empirical equation[12] developed earlier for bis(μ-hydroxo)-bridged dinuclear Cu(II) compounds, where the J value is a linear function of the Cu−O−Cu angle. The average Cu−O−Cu angle of 98.7° in the $Cu_2O_4N_2$ units of **4** would result in an approximate J value of -86 cm^{-1} according the empirical equation, comparable to the experimentally measured J_1 and J_2 values of -101 cm^{-1}. The calculated J value of -175 cm^{-1} for Krebs' compound which has an average Cu−O−Cu angle of 99.9° in the $Cu_2O_4N_2$ units is in agreement with the experimental value (-175 cm^{-1}). Such a good agreement could be attributed to the fact that the geometric parameters of the dinuclear units in **4** and Krebs' compound are similar to those of the bis(μ-hydroxo)-bridged dinuclear Cu(II) compounds employed in deriving the empirical equation; however, it could be also just a coincidence since the electronic structures of the μ-OH and μ_4-O ligands are clearly different.

The domination of antiferromagnetism in compound **4** makes it possible to investigate its solution behavior by ^{1}H NMR spectroscopy. The ^{1}H NMR spectra of **4** were recorded from 218 to 298 K in $CDCl_3$ (Figure 9). The spectrum at 218 K shows the chemical shifts of the methyl group on the phenyl ring (2.46 ppm), the phenyl (12.84 ppm), the methylene groups (20.86 ppm), and the methyl groups on the nitrogen atoms (42.75, 48.75 ppm). The low-temperature ^{1}H NMR spectrum of **4** is in agreement with the crystal structure. As shown in Figure 5, the molecule of **4** has an approximate C_2 symmetry. The two methyl groups on each nitrogen atom have different environments, one on the same side with the carboxylate oxygen atom occupying the fifth position of the copper center and the other on the opposite side, which resulted in the two methyl chemical shifts in the spectrum. For the same reason, the two protons of the methylene group also have different environments. The fact that only one chemical shift due to the CH_2 group was observed can be attributed to the broadness of the signals caused by the presence of paramagnetism. Upon the increase of temperature, the signals due to the phenyl (13.52 ppm at 298 K) and the methyl on the phenyl (3.35 ppm at 298 K) showed

(12) (a) Hatfield, W. E. In *Magneto-Structural Correlations in Exchange Coupled Systems*; Willett, R. D., Gatteschi, D., Kahn, O., Eds.; D. Reidel Publishing Co.: Dordrecht, The Netherlands, 1985; pp 554−602 and references therein. (b) Melnik, M. *Coord. Chem. Rev.* **1982**, *42*, 259. (c) Kato, M.; Muto, Y. *Coord. Chem. Rev.* **1988**, *92*, 45.

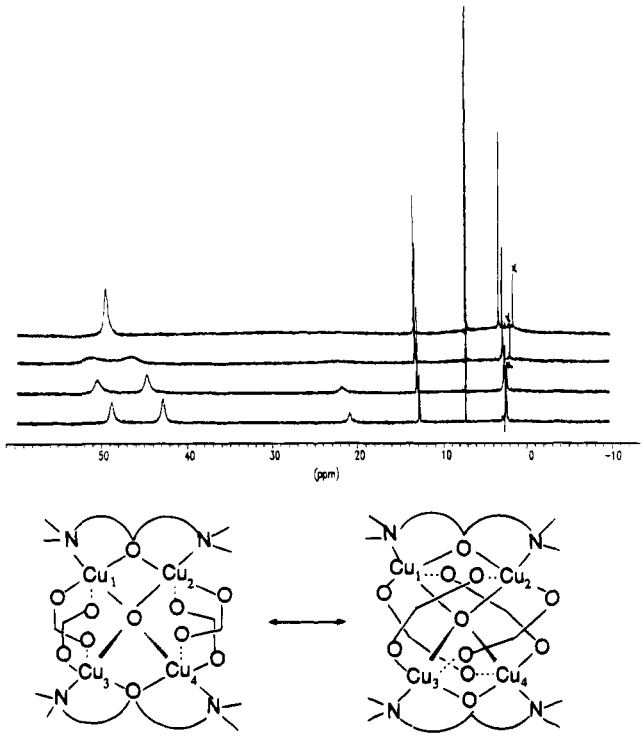

Figure 9. Top: Variable temperature ^1H NMR spectra of compound **4**. Bottom: A scheme illustrating the fluxional behavior of **4**.

a small degree of downfield shift while the CH_2 group (21.80 ppm at 233 K) and two methyl groups on the nitrogen displayed a substantial downfield shift (46.33 and 51.35 ppm, respectively, at 253 K). Such a downfield shift with the increase of temperature suggests that the ground state of compound **4** in solution is dominated by antiferromagnetism as well, consistent with the magnetism in the solid state.

In addition to the shift, the ^1H NMR spectra also revealed the fluxional behavior of **4**. With the increase of temperature, the signals due to the CH_2 and the CH_3 groups on nitrogen atoms broaden. At 298 K, only one signal of the CH_3 groups bound to the nitrogen atom is detected. The absence of the CH_2 signal at 298 K can be attributed to coalescence of the signal at this temperature. We believe that the fluxional behavior is caused by the switching of positions of the weakly bonded carboxylate oxygen atom between two copper centers, which can lead to the environment exchange of the two methyl groups on the nitrogen atom and the two protons of the CH_2 group as well (Figure 9). By using the chemical shifts at 218 K and the approximate coalescence temperature 260 K, the free energy of activation for this process was estimated to be about 11 kcal mol^{-1}.

Spectroscopic Studies and Electronic Structure of 1. Compound **1** is dark brown in solution and in the solid state. The reaction of compound **1** with $Pr(hfacac)_3$ does not produce any apparent color change. The UV–vis spectrum of **2** is complicated by the presence of intense absorption bands between 240 and 370 nm due to the hfacac ligand. In addition, the absorption maxima of compound **2** are concentration-dependent, which may be caused by a dissociation process of **2** in solution. Upon reaction of **1** with $La(O_2CCF_3)_3$, the brown-green color of **1** changed to green immediately. Since $La(O_2CCF_3)_3$ is colorless and the coordination environment of the Cu(II) ion in **3** is essentially identical with that in **1**, except that the oxygen atoms of the H_2O ligand and one of the bdmmp ligands

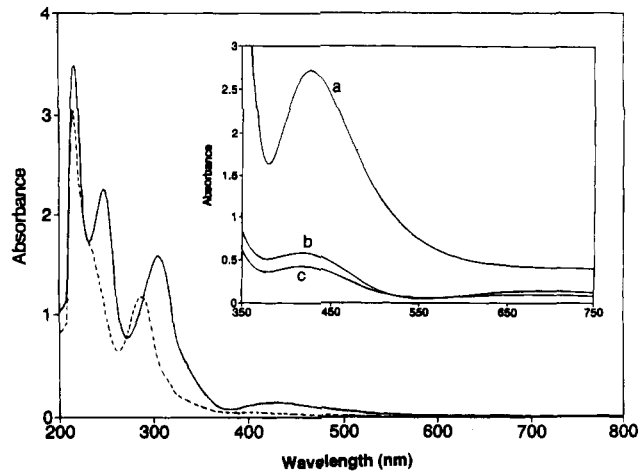

Figure 10. UV–vis spectra of compound **1** (solid line) and compound **3** (dashed line) in THF (1.25×10^{-4} M_{Cu}). Inset: (a) spectrum of compound **1** in THF (1.00×10^{-3} M); (b) spectrum 10 min after the addition of 1 equiv of $La(O_2CCF_3)_3$ to the solution of (a); (c) spectrum of compound **3** in THF (1.00×10^{-3} M_{Cu}).

coordinated to the Cu(II) ion in **1** are shared by both copper and lanthanide ions in **3**, we believe that the color change is caused by the La–O bond formation with the phenoxo and OH ligands. The reaction of compound **1** with $La(O_2CCF_3)_3$ was therefore monitored by a UV–vis spectrometer. As shown in Figure 10, compound **1** has three intense absorption bands in the UV–vis region located at $\lambda = 217$ nm ($\epsilon = 27\,840$ M^{-1} cm^{-1}), $\lambda = 247$ nm ($\epsilon = 18\,080$ M^{-1} cm^{-1}), and $\lambda = 305$ nm ($\epsilon = 12\,710$ M^{-1} cm^{-1}), characteristic of charge transfer bands, and a relatively weak absorption band at $\lambda = 427$ nm ($\epsilon = 1160$ M^{-1} cm^{-1}). Upon the addition of 1 equiv of $La(O_2CCF_3)_3$, the bands at 247, 305, and 427 nm shifted to shorter wavelengths with a substantial decrease of intensity ($\lambda = 233$ nm, $\epsilon \approx 13\,600$ M^{-1} cm^{-1}; $\lambda = 288$ nm, $\epsilon = 9440$ M^{-1} cm^{-1}; $\lambda = 422$ nm, $\epsilon = 460$ M_{Cu}^{-1} cm^{-1}), while the band at 217 nm experienced only a slight decrease of intensity ($\epsilon = 24\,320$ M_{Cu}^{-1} cm^{-1}). Because the coordination of the La(III) and Cu(II) ions to the bdmmp ligand could not have any significant effect on the electronic structure of the aromatic ring; hence the $\pi \rightarrow \pi^*$ transitions, but can influence the electron density and energy levels of the $p\pi$ electrons on the oxygen and nitrogen atoms, we suggest that the bands at 247, 305, and 427 nm are due to charge transfers involving the lone pairs of the nitrogen and oxygen atoms. The band at 427 nm must be due to the ligand → copper charge transfer because the free bdmmp ligand does not have any absorption bands in the visible region. The dramatic color change from brown to green in the formation of **2** can be attributed to the change of intensity of the 427 nm band. There is a very weak absorption band at about 680 nm in the spectra of **2** and **3** which is attributed to the d → d transitions.

In order to better understand the nature of the UV–vis absorption spectrum and the role of intramolecular hydrogen bonding for compound **1**, molecular orbital calculations were performed. These calculations were of the extended Hückel type[13] and employed the weighted H_{ij} formalism.[14] The molecular geometry employed for this calculation was taken directly from the crystal structural data with the 2-fold rotation axis placed along the z direction. The energy level diagram

(13) (a) Hoffmann, R. *J. Chem. Phys.* **1963**, *39*, 1397. (b) Hay, P. J.; Thibeault, J. L.; Hoffmann, R. J. *J. Am. Chem. Soc.* **1975**, *97*, 4884.
(14) (a) Ammeter, J. H.; Bürgi, H.-B.; Thibeault, J. L.; Hoffmann, R. *J. Am. Chem. Soc.* **1978**, *100*, 3686. (b) Mealli, C.; Proserpio, D. M. *J. Chem. Educ.* **1990**, *67*, 399.

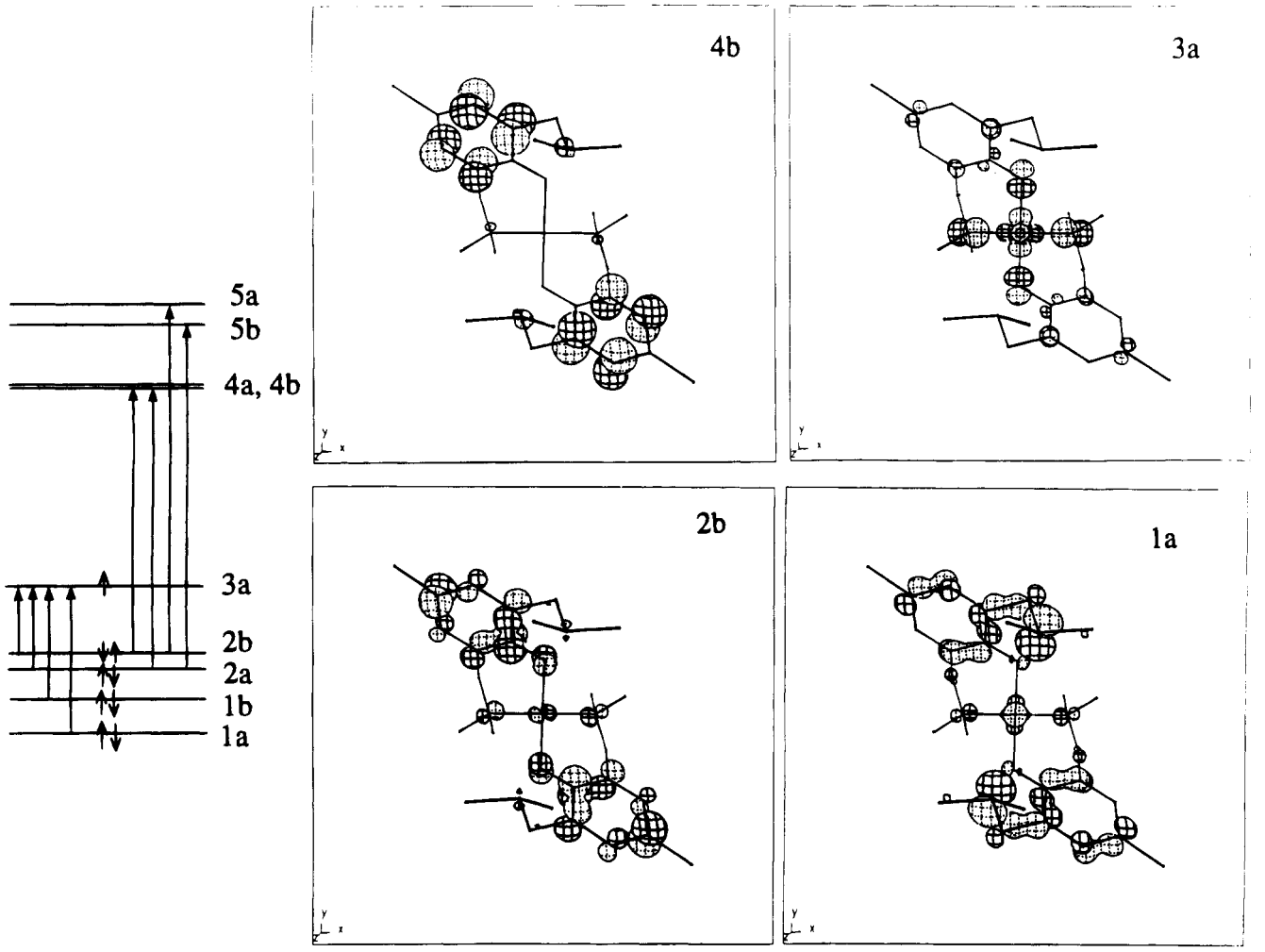

Figure 11. Energy level diagram of **1** and plots of selected frontier orbitals projected down the z axis (the H_2O—Cu vector).

Table 4. UV—Vis Absorption Assignments

abs λ, nm	assignment
217	2a → 5a (5b), 2b → 5a (5b) ($\pi \rightarrow \pi^*$)
247	2a → 4a (4b) ($\pi \rightarrow \pi^*$)
305	2b → 4a (4b) ($\pi \rightarrow \pi^*$)
427	1a → 3a, 1b → 3a (N lone pair → Cu $d_{x^2-y^2}$)
	2a → 3a, 2b → 3a (π → Cu $d_{x^2-y^2}$)

and electron density plots of selected frontier orbitals are shown in Figure 11. Orbitals 4a, 4b, 5b, and 5a are the π^* orbitals of the phenyl. Orbitals 2a and 2b are the π orbitals involving the phenyl ring and the phenoxy oxygen atom, while orbitals 1a and 1b are essentially the lone pair orbitals of the uncoordinated nitrogen atoms. The arrows on the energy level diagram in this figure correspond to the assignments of the four observed transitions in the UV—vis spectrum of **1** which are described in detail in Table 4.

From Table 4 it can be seen that the absorption maximum occurring at 427 nm in compound **1** is most likely of a multicomponent nature. The four components of this transition arise due to the charge transfer from orbitals with phenoxy π character or the uncoordinated nitrogen lone pair character to the singly occupied copper $d_{x^2-y^2}$ orbital. It is most likely that the contribution from the lone pair orbitals of nitrogen atoms is nominal due to the low transition moment between atoms which are not directly bonded. Upon reaction with $La(O_2CCF_3)_3$, all contributions to this band from the nitrogen lone pairs and one of the phenoxy oxygen atoms disappear, which leads to a decrease in the intensity for this absorption (Figure 10). The shifts of the bands at 305 and 247 nm are most likely

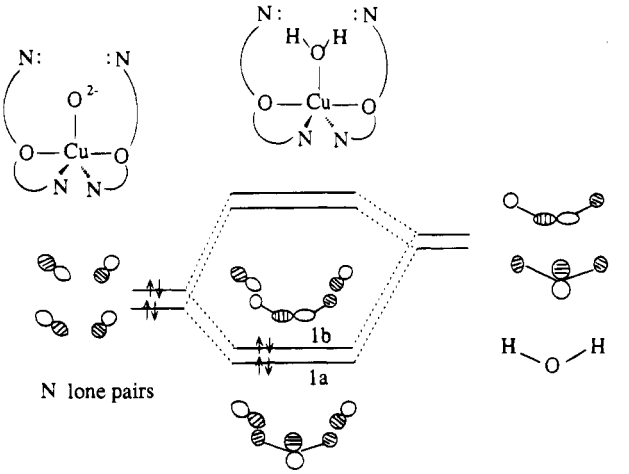

Figure 12. Correlation diagram showing the effect of hydrogen bonding on the lone pairs of the two uncoordinated nitrogen atoms in **1**.

due to the conversion of the terminal phenoxy group to a bridging phenoxy ligand upon reaction with the lanthanide complexes. As this reaction will reduce the basicity of the oxygen electrons (therefore a lowering in energy), a blue shift will be observed for the absorption maxima associated with this ligand.

The effect of the hydrogen bonding between the water molecule and the uncoordinated nitrogen lone pairs on the bdmmp ligands was investigated by a EHMO calculation

replacing the water molecule with a terminal oxide with a Cu−O^{2-} bond equal to the Cu−OH_2 bond in **1**. The major difference in energy levels for the frontier orbitals between compound **1** and the oxide compound is associated with the two orbitals involving mostly the nitrogen lone pairs. These two orbitals in the oxide compound are destabilized by about 0.05 eV with an increased nitrogen p orbital contribution and a decrease in the oxygen s and p orbital contribution. This is a result of the loss of overlap between the nitrogen atoms and the O−H σ^* orbitals of H_2O, which stabilizes the energy of the nitrogen orbitals and at the same time increases the energy of the oxygen by back-donation of electron density into the O−H σ^* orbital in **1**. In short, the effect of the intramolecular hydrogen bonding in **1** is to increase the basicity at the oxygen at H_2O at the expense of the two amino groups of the bdmmp ligand (Figure 12).

Acknowledgment. We thank the NSERC (Canada) for financial support, Professor Pierre D. Harvey for his assistance in EHMO calculations, and Mr. Mike Fuerth for his assistance in recording the NMR spectra of **4**.

Supplementary Material Available: Tables listing experimental data for X-ray diffraction analyses and complete atomic coordinates, anisotropic thermal parameters, bond lengths, and bond angles for all four compounds (45 pages). Ordering information is given on any current masthead page.

IC9405642